



Telling, J., Eric, B., Bone, N., EL, J., Tranter, M., MacFarlane, J., ... DA, H. (2015). Rock comminution as a source of hydrogen for subglacial ecosystems. *Nature Geoscience*, 8, 851-855. [NGEO2533]. DOI: 10.1038/NGEO2533

Peer reviewed version

License (if available):  
Unspecified

Link to published version (if available):  
[10.1038/NGEO2533](https://doi.org/10.1038/NGEO2533)

[Link to publication record in Explore Bristol Research](#)  
PDF-document

This is the accepted author manuscript (AAM). The final published version (version of record) is available online via Nature Publishing Group at <http://dx.doi.org/10.1038/ngeo2533>. Please refer to any applicable terms of use of the publisher.

## University of Bristol - Explore Bristol Research

### General rights

This document is made available in accordance with publisher policies. Please cite only the published version using the reference above. Full terms of use are available:  
<http://www.bristol.ac.uk/pure/about/ebr-terms.html>

## **Rock comminution as a source of hydrogen for subglacial ecosystems**

**J. Telling<sup>1\*</sup>, E.S. Boyd<sup>2</sup>, N. Bone<sup>1</sup>, E.L. Jones<sup>1</sup>, M. Tranter<sup>1</sup>, J.W. MacFarlane<sup>3</sup>, P.G. Martin<sup>3</sup>, J.L. Wadham<sup>1</sup>, G. Lamarche-Gagnon<sup>1</sup>, M.L. Skidmore<sup>4</sup>, T.L. Hamilton<sup>5</sup>, E. Hill<sup>6</sup>, M. Jackson<sup>7</sup> and D.A. Hodgson<sup>8</sup>**

<sup>1</sup>School of Geographical Sciences, University of Bristol, University Road, Bristol, BS8 1SS, UK

<sup>2</sup>Department of Microbiology and Immunology, Montana State University, Bozeman, MT 59717, USA

<sup>3</sup>Interface Analysis Centre, School of Physics, University of Bristol, 121 St Michael's Hill, Bristol, BS8 1TL, UK

<sup>4</sup>Department of Earth Sciences, Montana State University, Bozeman, MT 59717, USA

<sup>5</sup>Department of Biological Sciences, University of Cincinnati, Cincinnati, OH, 45221, USA

<sup>6</sup>Natural Resources Laboratory, Carl Zeiss Microscopy Ltd, 509 Coldhams Lane, Cambridge, CB1 3JS UK

<sup>7</sup>Norwegian Water Resources & Energy Directorate, Hydrology Department; Glacier, Snow and Ice Section, N-0301 Oslo, Norway

<sup>8</sup>British Antarctic Survey, Madingley Road, High Cross, Cambridge, CB3 0ET

\*email: [jon.telling@bristol.ac.uk](mailto:jon.telling@bristol.ac.uk)

**Substantial parts of the beds of glaciers, ice sheets, and ice caps are at the pressure melting point<sup>1</sup>. The resulting water harbours diverse subglacial microbial ecosystems<sup>2,3</sup> capable of affecting global biogeochemical cycles<sup>4,5</sup>. Such subglacial habitats may have acted as refugia during Neoproterozoic glaciations<sup>6</sup>. However, it is unclear how life in subglacial**

**environments could be supported during glaciations lasting millions of years because energy from overridden organic carbon would become increasingly depleted<sup>7,8</sup>. Here we investigate the potential for abiogenic H<sub>2</sub> produced during rock comminution to provide a continual source of energy to support subglacial life. We collected a range of silicate rocks representative of subglacial environments in Greenland, Canada, Norway, and Antarctica and crushed them with a sledgehammer and ball mill to varying surface areas. Under an inert atmosphere in the lab, we added water, and measured H<sub>2</sub> production with time. H<sub>2</sub> was produced at 0°C in all silicate-water experiments, probably via the reaction of water with mineral surface silica radicals formed during rock comminution. H<sub>2</sub> production increased with increasing temperature or decreasing silicate rock grain size. Sufficient H<sub>2</sub> was produced to support previously measured rates of methanogenesis under a Greenland glacier. We conclude that abiogenic H<sub>2</sub> generation from glacial bedrock comminution could have supported life and biodiversity in subglacial refugia during past extended global glaciations.**

Once thought sterile, subglacial habitats are now known to harbour genetically and functionally diverse microbial ecosystems capable of accelerating rock weathering<sup>9</sup>, affecting global carbon cycles<sup>4</sup>, and influencing productivity in adjacent oceans<sup>5</sup>. During extended global Neoproterozoic glaciations, ice sheets may have covered the Earth's continents for millions of years with substantial sectors at the pressure melting point<sup>10</sup>.

It has been proposed that subglacial environments may have acted as refugia for the survival of microorganisms during extensive Neoproterozoic glaciations<sup>6</sup>, helping to preserve the diversity of prokaryotes and lower order eukaryotes<sup>3,6</sup>. It is not clear how subglacial ecosystems could be supported over glaciations spanning millions of years, however, since reserves of overridden photosynthetically derived carbon (e.g. soils, vegetation) would become depleted<sup>7,8</sup>.

Water-rock chemolithotrophic reactions could provide additional sources of energy to sustain subglacial ecosystems<sup>11</sup>. Abiogenic H<sub>2</sub>, formed by a variety of water-rock reactions including serpentinization<sup>12,13</sup>, radiolysis<sup>14</sup> or mineral surface radical reactions<sup>15</sup>, provides an energy substrate for a variety of warm to hot ( $\geq 22^{\circ}\text{C}$ ) subsurface environments. No abiogenic H<sub>2</sub> generating experiments have, however, focused on temperatures relevant to subglacial environments ( $0^{\circ}\text{C}$  to  $-2.5^{\circ}\text{C}$ , dependent on overlying ice thickness<sup>1</sup>). Here we test the hypothesis that abiogenic H<sub>2</sub> can be produced from rock-water reactions at  $0^{\circ}\text{C}$  in sufficient quantities to be able to support subglacial microbial activity.

The ability of six silicate rock types samples from glacial catchments (gneiss, quartzite, shale, granite, nepheline-syenite, schist) to generate abiogenic H<sub>2</sub> in water-rock reactions were tested. Calcite was used as a non-silicate control. The molar compositions of the starting materials are given in Supplementary Table S1. The rocks and mineral control were crushed to a range of different surface areas under an inert atmosphere, wetted with water, and the generation of H<sub>2</sub> followed over time.

All six silicate rock types produced H<sub>2</sub> when crushed and wetted with water at  $0^{\circ}\text{C}$  (Figure 1). There was no detectable H<sub>2</sub> generation in experiments with calcite ( $< 2.7 \text{ nmol H}_2 \text{ g}^{-1}$ ) (Figure 2). Grain size and surface area were weakly inversely correlated ( $R^2 = -0.29$ ,  $n = 30$ ,  $p < 0.001$ ; Figure 1a). The production of H<sub>2</sub> was significantly correlated with total surface area ( $R^2 = 0.53$ ,  $n = 60$ ,  $p < 0.001$ , Figure 1b), with a stronger correlation when surface area was normalised to molar silica content ( $R^2 = 0.70$ ,  $n = 60$ ,  $p < 0.001$ , Figure 1c). There was a weaker correlation with number of surface radicals ( $R^2 = 0.20$ ,  $n = 60$ ,  $p < 0.001$ , Figure 1d). These data provide the first evidence for abiogenic production of H<sub>2</sub> at  $0^{\circ}\text{C}$ , i.e. temperatures relevant to subglacial environments. The strong correlation between silica surface area and H<sub>2</sub> generation coupled with the detection of surface radicals on the surface of crushed natural silicate rocks is consistent with H<sub>2</sub> generation via the reaction of silica surface radicals with

water (Equations 1 and 2)<sup>15</sup>, with the free radicals formed through the shearing of surface mineral bonds during subglacial rock comminution. We note that free radicals were not detected in our crushed calcite, consistent with a lack of detectable H<sub>2</sub> in these control experiments.



Silica radical-water reactions have previously been postulated to produce H<sub>2</sub> in active fault zones at higher temperatures (25-300°C) (Equations 1 and 2)<sup>15,16</sup>. The rate of H<sub>2</sub> production when crushed rock was added to water decreased after 24 hours (Figure 2, Figure 3), consistent with previous experiments at temperatures of 35°C and above<sup>16</sup> and the known stability of some silica surface radicals of several days to weeks<sup>17</sup>. For all three silicate rocks tested, rates of H<sub>2</sub> generation were similar at 0°C and 10°C, but higher at 35°C (Figure 2). This temperature dependence may be due to the transformation of more stable SiO• radicals to more reactive Si• radicals at higher temperatures<sup>15</sup>.

The amount of experimental H<sub>2</sub> generated likely underestimated *in situ* abiogenic H<sub>2</sub> subglacial production, for the following reasons. First, the shape of many of the H<sub>2</sub> generation curves in Figures 2 and 3 suggest that production may continue for longer than the 120 hour experimental period. Second, it is likely that less stable surface radicals will be lost during and after dry crushing, prior to the addition of water. Third, H<sub>2</sub> may be produced by additional water-rock interactions such as serpentinization<sup>12,13</sup>, although these are untested at subglacially relevant temperatures. Finally, additional H<sub>2</sub> could have been released from fluid inclusions<sup>18</sup> during the initial dry crushing stage of our methods.

Our experimental data suggests that the amount of H<sub>2</sub> generated from subglacial rock comminution depends primarily on the rate of rock abrasion, the presence of liquid water, and

the underlying silicate lithology (Figure 1). Subglacial rock erosion takes place through a combination of plucking, abrasion, and chemical dissolution<sup>19</sup>. Of these, abrasion is the key process for producing the fine grained glacial flour that is the dominant source of suspended sediments in glacial rivers<sup>19</sup>, and which would provide the substrate for most subglacial H<sub>2</sub> generation because of its high surface area and large number of exposed silica radicals<sup>15</sup>. Those sectors of glaciers and ice sheets with liquid water at the bed typically have higher rates of erosion due to increased lubrication for sliding, greatly enhancing the ability of rocks entrained into basal ice to abrade underlying rocks and sediment<sup>19,20</sup>. Rates of modern glacial erosion vary by four orders of magnitude, from 0.01 mm yr<sup>-1</sup> for cold-based polar glaciers and ice sheets, up to 100 mm yr<sup>-1</sup> for fast moving, temperate glaciers<sup>21</sup>.

We crudely estimated the catchment scale H<sub>2</sub> generation by rock comminution for one of our study sites; the 600 km<sup>2</sup> Leverett Glacier, SW Greenland. We first used the regression equation in Figure 1c to calculate the potential H<sub>2</sub> that could be generated from silica radical-water reactions, using the measured mean molar silica surface area of suspended sediment from the catchment (Methods). We then scaled up our calculations using measurements of the annual suspended sediment flux from the glacier<sup>22</sup> (Methods). We calculated that 150 nmoles H<sub>2</sub> m<sup>-2</sup> d<sup>-1</sup> would be produced from rock comminution under the glacier. We further estimated that the release of trapped palaeoatmospheric gases (O<sub>2</sub>, CO<sub>2</sub>) from basal ice melt could provide sufficient electron acceptors to quantitatively utilize this H<sub>2</sub> (Methods), depending on the competing demands of other reductants such as organic matter or metal sulphides. Additional electron acceptors could derive from basal ice melt (e.g. NO<sub>3</sub><sup>-</sup>) or mineral weathering reactions (e.g. SO<sub>4</sub><sup>2-</sup>, Fe<sup>3+</sup>)<sup>23</sup>.

H<sub>2</sub> is a labile energy substrate for a wide range of microorganisms, and is likely to be readily utilized if sufficient electron acceptors are available<sup>24</sup>. A variety of studies provide compelling evidence that abiogenic H<sub>2</sub> produced during rock comminution can be utilized by

subglacial microorganisms. A range of aerobic and anaerobic bacteria inferred to be capable of oxidizing H<sub>2</sub> as a source of energy have been identified in subglacial sediments, including strains of *Thiobacillus*, *Rhodospirillum rubrum*, *Geobacter*<sup>3</sup>, and a diversity of methanogens<sup>8,25</sup>. Prior studies on subglacial microbial activity have focused on methanogens, due to the importance of methane released to the atmosphere as a greenhouse gas<sup>4,8</sup>. Our H<sub>2</sub> production rate from rock comminution is 10× more than potentially required to support measured rates of methanogenesis in the upper centimetre of subglacial sediment at Russell Glacier<sup>8</sup>, a glacier immediately adjacent to Leverett Glacier and overriding similar bedrock (Methods). Furthermore, rates of methanogenesis in these subglacial sediments increased 10× with the addition of excess H<sub>2</sub> at 1°C<sup>8</sup>, with 16S rRNA gene diversity data consistent with methanogens capable of hydrogenotrophy<sup>8</sup>. At Robertson Glacier (Canada), where rates of subglacial methanogenesis were similar to those at Russell Glacier<sup>25</sup>, H<sub>2</sub> again accelerated microbial CH<sub>4</sub> production and increased the abundance of a unique methanogen phylotype that was prevalent in subglacial sediment (Figures S1, S2 and S3 in Supplementary Information). Finally, carbon isotopic values of methane from the base of the GRIP and GISP2 ice cores in the centre of the Greenland ice sheet are consistent with microbial hydrogenotrophic pathways<sup>26,27</sup>.

The only subglacial H<sub>2</sub> concentrations reported to date are from refrozen waters at the base of the NGRIP core from near the centre of the Greenland ice sheet<sup>28</sup>. H<sub>2</sub> concentrations were 200-550 nM<sup>28</sup>, higher than the 1-10 nM range typical of terrestrial groundwaters<sup>29</sup> and more consistent with abiogenic H<sub>2</sub> from hydrothermal hot springs<sup>30</sup>. Such high concentrations could plausibly be produced by silica radical reactions. If a gram of Greenland gneiss is crushed to a surface area of 4.37 m<sup>2</sup> g<sup>-1</sup> (Table S2) in a 1:1 volume mix with pore water, 11.4 nmoles H<sub>2</sub> g<sup>-1</sup> would be generated (Figure 1c), resulting in a dissolved H<sub>2</sub> concentration of 11,400 nM; over an order of magnitude more than measured at the base of the NGRIP core. This suggests

that H<sub>2</sub> generation could potentially outstrip the supply of electron acceptors from basal ice melt and mineral weathering beneath the interior of ice sheets.

The importance of abiogenic H<sub>2</sub> generation in sustaining subglacial communities will additionally depend on the concentration and bioavailability of other energy substrates under the ice, in particular organic matter. H<sub>2</sub> generated from rock comminution is likely to be a significant microbial energy substrate beneath wet based glaciers and ice sheets with little bioavailable organic matter, and/or over glaciations where isolation ages from the surface are long enough for microorganisms to utilize the majority of labile organic matter. Where glaciers have recently overridden labile organic matter, or where moulins allow surface organic matter to be transported to the base of the ice, the impact of abiogenic H<sub>2</sub> on subglacial ecosystems is likely to be overwhelmed by heterotrophic microbial activity. As an example, rates of methanogenesis at a glacier which had recently overridden fresh algal mats (John Evans Glacier, Ellesmere Island) were orders of magnitude greater<sup>8</sup> than more refractory organic carbon sediments at Russell and Robertson Glaciers<sup>8,25</sup>, with rates of methanogenesis stimulated not by H<sub>2</sub> but by acetate indicating the presence of acetoclastic methanogens<sup>8</sup>.

Thick glacial deposits (up to a kilometre thick) with abundant evidence of glacial scouring and abrasion indicate active hydrological cycles and significant rates of erosion under wet based ice sheets during Neoproterozoic ice ages that lasted millions of years<sup>10</sup>. H<sub>2</sub> generated through rock comminution provides a mechanism for supporting continued microbial metabolism in extensive subglacial refugia after relict photosynthetic organic carbon has been depleted during long glaciations. Modern studies demonstrate that subglacial environments are genetically diverse<sup>3</sup>, and that subglacial outflows from the Antarctic ice sheet provide an important source of nutrients and microbes to the Southern Ocean<sup>5</sup>. By analogy, subglacial habitats may have been important reservoirs of microbial diversity during



Neoproterozoic glaciations, with subglacial water providing fluxes of nutrients and genes to the Neoproterozoic marine environment.

## References

- 1 Bell, R. E. The role of subglacial water in ice-sheet mass balance. *Nature Geoscience* **1**, 297-304 (2008).
- 2 Christner, B. C. *et al.* A microbial ecosystem beneath the West Antarctic ice sheet. *Nature* **512**, 310-313 (2014).
- 3 Hamilton, T. L., Peters, J. W., Skidmore, M. L. & Boyd, E. S. Molecular evidence for an active endogenous microbiome beneath glacial ice. *ISME Journal* **7**, 1402-1412 (2013).
- 4 Wadham, J. L. *et al.* Potential methane reservoirs beneath Antarctica. *Nature* **488**, 633-637 (2012).
- 5 Death, R. *et al.* Antarctic ice sheet fertilises the Southern Ocean. *Biogeosciences* **11**, 2635-2643 (2014).
- 6 Christner, B. C., Skidmore, M.L., Priscu, J.C., Tranter, M. & Foreman, C.M. *Psychrophiles: from Biodiversity to Biotechnology* Ch. 4 (Springer, Berlin, 2008).
- 7 Moczydlowska, M. The Ediacaran microbiota and the survival of Snowball Earth conditions. *Precambrian Research* **167**, 1-15 (2008).
- 8 Stibal, M. *et al.* Methanogenic potential of Arctic and Antarctic subglacial environments with contrasting organic carbon sources. *Global Change Biology* **18**, 3332-3345 (2012).

- 9 Montross, S. N., Skidmore, M., Tranter, M., Kivimaki, A.-L. & Parkes, R. J. A microbial driver of chemical weathering in glaciated systems. *Geology* **41**, 215-218 (2013).
- 10 Hoffman, P. F. & Schrag, D. P. The snowball Earth hypothesis: testing the limits of global change. *Terra Nova* **14**, 129-155 (2002).
- 11 Boyd, E. S., Hamilton, T. L., Havig, J. R., Skidmore, M. L. & Shock, E. L. Chemolithotrophic Primary Production in a Subglacial Ecosystem. *Applied Environmental Microbiology* **80**, 6146-6153 (2014).
- 12 Kelley, D. S. *et al.* A serpentinite-hosted ecosystem: The lost city hydrothermal field. *Science* **307**, 1428-1434 (2005).
- 13 Stevens, T. O. & McKinley, J. P. Lithoautotrophic microbial ecosystems in deep basalt aquifers. *Science* **270**, 450-454 (1995).
- 14 Lin, L. H. *et al.* Radiolytic H<sub>2</sub> in continental crust: Nuclear power for deep subsurface microbial communities. *Geochemistry Geophysics Geosystems* **6**, Q07003 (2005).
- 15 Kita, I., Matsuo, S. & Wakita, H. H<sub>2</sub> generation by reaction between H<sub>2</sub>O and crushed rock - an experimental study on H<sub>2</sub> degassing from the active fault zone. *Journal of Geophysical Research* **87**, 789-795 (1982).
- 16 Sugisaki, R. *et al.* Origin of hydrogen and carbon dioxide in fault gases and its relation to fault activity. *Journal of Geology* **91**, 239-258 (1983).
- 17 Fubini, B., Bolis, V., Cavenago, A. & Volante, M. Physicochemical properties of crystalline silica dusts and their possible implication in various biological responses. *Scandinavian Journal of Work, Environment & Health* **21**, 9-14 (1995).
- 18 Konnerup-Madsen, J. & Rosehansen, J. Volatiles associated with alkaline igneous rift activity – fluid inclusions in the Ilimaussaq intrusion and the Gardar granitic complexes (South Greenland). *Chemical Geology* **37**, 79-93 (1982).

- 19 Hallet, B. A theoretical model of glacial abrasion. *Journal of Glaciology* **23**, 39-50 (1979).
- 20 Zoet, L. K., Alley, R. B., Anandakrishnan, S. & Christianson, K. Accelerated subglacial erosion in response to stick-slip motion. *Geology* **41**, 159-162 (2013).
- 21 Hallet, B., Hunter, L. & Bogen, J. Rates of erosion and sediment evacuation by glaciers: A review of field data and their implications. *Global and Planetary Change* **12**, 213-235 (1996).
- 22 Hawkings, J. R. *et al.* Ice sheets as a significant source of highly reactive nanoparticulate iron to the oceans. *Nature Communications* **5**, 3929-3929 (2014).
- 23 Tranter, M., Skidmore, M. & Wadham, J. Hydrological controls on microbial communities in subglacial environments. *Hydrological Processes* **19**, 995-998 (2005).
- 24 Thauer, R. K., Jungermann, K. & Decker, K. Energy conservation in chemotrophic anaerobic bacteria. *Bacteriological Reviews* **41**, 100-180 (1977).
- 25 Boyd, E. S., Skidmore, M., Mitchell, A. C., Bakermans, C. & Peters, J. W. Methanogenesis in subglacial sediments. *Environmental Microbiology Reports* **2**, 685-692 (2010).
- 26 Souchez, R. *et al.* Gas isotopes in ice reveal a vegetated central Greenland during ice sheet invasion. *Geophysical Research Letters* **33**, L24503 (2006).
- 27 Miteva, V., Teacher, C., Sowers, T. & Brenchley, J. Comparison of the microbial diversity at different depths of the GISP2 Greenland ice core in relationship to deposition climates. *Environmental Microbiology* **11**, 640-656 (2009).
- 28 Christner, B. C., Montross, G. G. & Priscu, J. C. Dissolved gases in frozen basal water from the NGRIP borehole: implications for biogeochemical processes beneath the Greenland Ice Sheet. *Polar Biology* **35**, 1735-1741 (2012).

- 29 Lovley, D. R. & Goodwin, S. Hydrogen concentrations as an indicator of the predominant terminal electron-accepting reactions in aquatic sediments. *Geochimica et Cosmochimica Acta* **52**, 2993-3003 (1988).
- 30 Spear, J. R., Walker, J. J., McCollom, T. M. & Pace, N. R. Hydrogen and bioenergetics in the Yellowstone geothermal ecosystem. *Proceedings of the National Academy of Sciences of the United States of America* **102**, 2555-2560 (2005).

**Author information.** Correspondence and requests for materials should be addressed to J.T. (jon.telling@bristol.ac.uk).

**Acknowledgements.** The authors acknowledge funding from an E.U. INTERACT Transnational Access grant (to JT), NASA Exobiology and Evolutionary Biology program (NNX10AT31G to MLS and ESB) and the NASA Astrobiology Institute (NNA15BB02A to ESB).

**Author Contributions.** J.T. conceived and designed the project. E.S.B. oversaw the microbiological analyses. N.B., E.L.J., G.L.-G., P.G.M. and J.W.M. performed the experiments and geochemical analyses. T.L.H. performed the microbiological experiments and analyses. M.L.S., M.J., D.A., E.H. and J.L.W. contributed materials. E.H. assisted on fieldwork. J.T., E.S.B., N.B., M. T., J.L.W. and M.L.S. co-authored the paper.

**Competing Financial Interests.** There are no competing financial interests.

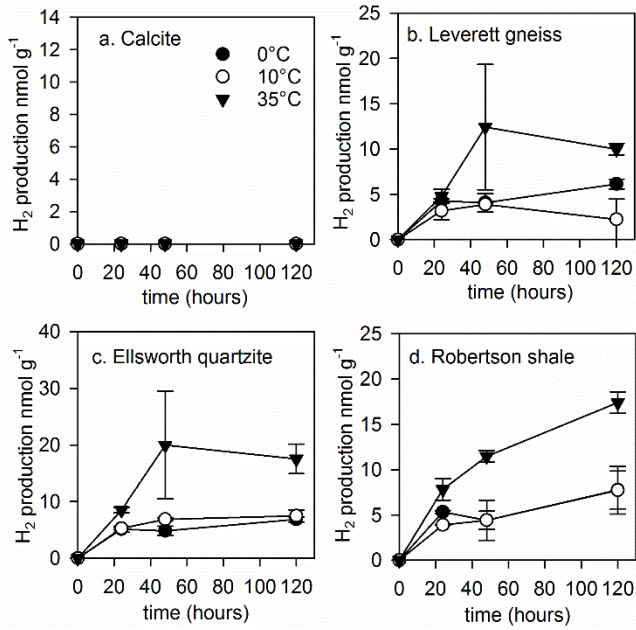
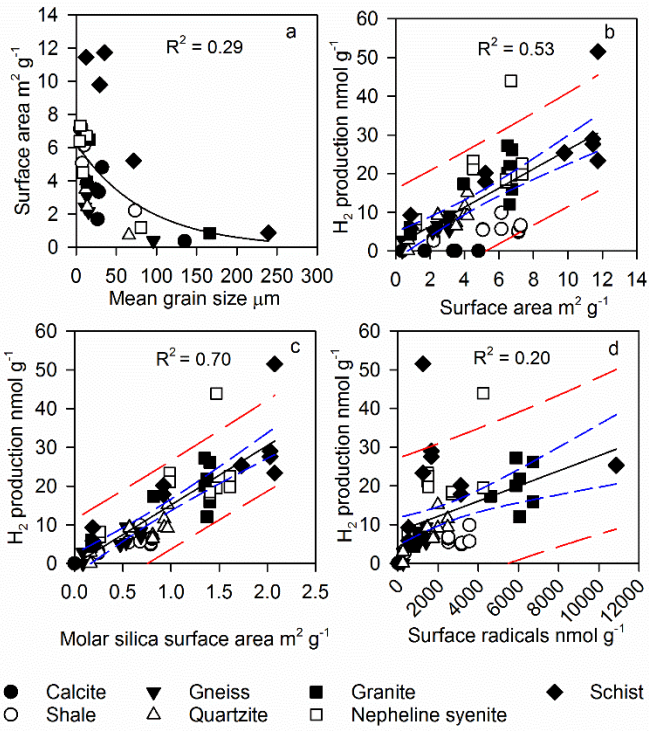
## Figure Legends

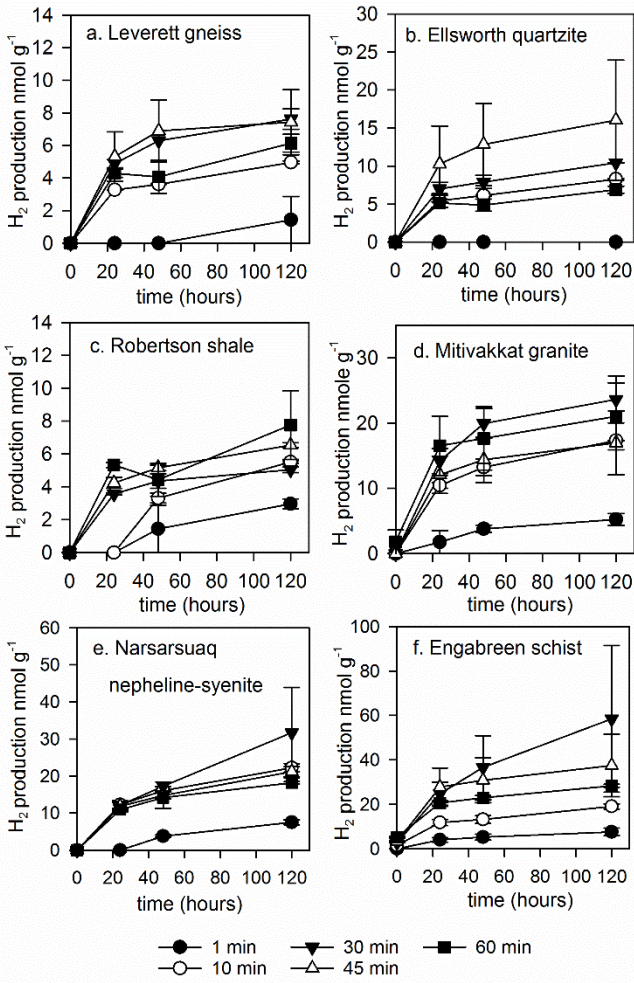
**Figure 1. Results of rock and mineral comminution experiments at 0°C.** **a**, grain size versus surface area for crushed silicate rocks and calcite. **b**, Surface area against H<sub>2</sub> generation. **c**,

Molar silica surface area against H<sub>2</sub> generation. **d**, Number of surface radicals against H<sub>2</sub> generation. Solid black lines show regression lines, short dashed lines show 95% confidence limits on regression lines, and outer dashed-dot lines show 95% confidence limits for predicting y values from x. The best fit equation in Figure 1c is  $y = 15.34x - 0.19$ . Calcite was excluded for regression analysis in b, c and d.

**Figure 2.** Gaseous H<sub>2</sub> generation during rock comminution of three tested silicate rocks as a function of three different temperatures. Symbols show the mean of duplicate samples, with individual sample values represented by the length of error bars.

**Figure 3.** Temporal variation of gaseous H<sub>2</sub> production from crushed calcite (non-silicate control) and silicate rocks. The symbols indicate the mean values of duplicate samples with different grinding times (see key) and hence different surface areas. Individual sample values are represented by the length of error bars.





## **Rock comminution as a source of hydrogen for subglacial ecosystems**

**J. Telling<sup>1\*</sup>, E.S. Boyd<sup>2</sup>, N. Bone<sup>1</sup>, E.L. Jones<sup>1</sup>, M. Tranter<sup>1</sup>, J.W. MacFarlane<sup>3</sup>, P.G. Martin<sup>3</sup>, J.L. Wadham<sup>1</sup>, G. Lamarche-Gagnon<sup>1</sup>, M.L. Skidmore<sup>4</sup>, T.L. Hamilton<sup>5</sup>, E. Hill<sup>6</sup>, M. Jackson<sup>7</sup> and D.A. Hodgson<sup>8</sup>**

### **METHODS**

#### **Rock comminution experiments**

Representative rocks (gneiss, calcareous shale, quartzite, granite, nepheline-syenite, schist) were sampled from six different glacial catchments (Leverett Glacier, SW Greenland; Robertson Glacier, Canada; Ellsworth Mountains, Antarctica; Mitivakkat Glacier, E Greenland; Kiattuut Sermiat Glacier, S. Greenland; Engabreen, Norway). Pure calcite (Morocco) was purchased from the Geology Superstore ([www.geologysuperstore.com](http://www.geologysuperstore.com)). Starting rock and mineral samples were washed in 18.2 M $\Omega$  cm<sup>-1</sup> water, and dried at 100°C for two days. Samples were then placed in multiple thick polyethylene bags (to avoid metal-rock interaction) and crushed with a sledge hammer on a metal plate. Samples were sieved, and the 250  $\mu$ m to 2 mm size fraction collected and dried at 100°C for two days prior to milling. Crushed materials were then ground to a variety of surface areas under 5.0 grade Ar in a gas-tight agate ball mill in a Fritsch Planetary Mono Mill Pulverisette 6 at 500 rpm for different times (1-60 minutes). 10 g of material were used for the 1 to 45 minutes crushing times, and 30 g fractions were used for the final 60 minute crushing time. After milling, materials were transferred to a glove bag filled and continually flushed with 5.0 grade Ar, and 3 g sub-fractions transferred into 20 ml borosilicate serum vials (previously acid washed, rinsed 6 $\times$  with 18.2 M $\Omega$  cm<sup>-1</sup> water, and furnace at 450°C). Vials were sealed with thick butyl rubber stoppers (previously boiled in 1M NaOH for 1hr and rinsed 6 $\times$  with 18.2 M $\Omega$  cm<sup>-1</sup> water), and crimp sealed. Vial headspaces were flushed with 5.0 grade Ar for 2 minutes to remove any traces of



oxygen. At the start of experiments, an initial headspace sample was taken by adding 5 ml of 5.0 grade Ar, and removing a 5 ml sample using a gastight syringe. 3 ml of anoxic water (sparged with Ar for >1 hour) was then added to the vials using a syringe and needle. Samples were shaken gently for 1 minute to ensure mixing of water and crushed material, then 5 ml gas samples removed as before, replacing with 5.0 grade Ar. Samples were then incubated at various temperatures (0°C, 10°C, 35°C), with further gas samples taken at 24, 48 and 120 hours.

Gas samples were analysed on an Agilent 7980A gas chromatograph, using a 1 ml sample loop. H<sub>2</sub> separation was achieved using a Hayesep D 80-100 mesh, 2m x 1/8 inch SS column, in series with a molecular sieve 5a, 60-80 mesh, 8ft x 1/8 inch column at a temperature of 25°C. Sample concentrations were calculated from careful multiple manual dilution of a certified ( $\pm$  5%) 493 ppm standard in 5.0 grade Ar flushed 100 ml serum vials (linear over 5 ppm to 493 ppm calibration range,  $R^2 = 0.999$ ,  $n = 5$ ). Standards run daily throughout the experimental period gave a coefficient of variation for H<sub>2</sub> of 2.7% ( $n = 38$ ), with a detection limit of 5 ppm, equivalent to 2.7 nmol g<sup>-1</sup>. Gas concentrations were converted to molar concentrations using the ideal gas law, corrected for water dissolution<sup>1</sup>, and normalised to dry sediment mass.

The surface area of materials was measured using a NOVA 1200e BET Analysis System using nitrogen gas as an adsorbant at 77K. The mean, minimum and maximum percentage variation for duplicate measurements were 5.0%, 0.1% and 6.8% respectively. Grain size was measured on a Malvern Mastersizer 3000, based on laser diffraction, with 5 replicates per sample. The mean, minimum and maximum percentage variation for 5 replicate measurements were 4.4%, 0.3% and 19.2 % respectively ( $n=30$ ). Elemental composition was quantified using energy dispersive X-ray spectroscopy, using a Zeiss Gemini Sigma VP system fitted with an EDAX Octane Silicon Drift detector. Spectrum analyses were taken at random

points across small (< 0.1g) samples, and compositions calculated from the mean. Texture and Elemental Analytical Microscopy software was used for post processing and error estimation, with an average percentage variation between 5 replicate samples of 12%. The number of reactive surface radicals on starting materials was estimated using a UV absorbance method, by quantifying the bleaching of the radical scavenger molecule 2,2-diphenyl-1-picrylhydazyl (DPPH)<sup>2</sup>. After sparging a 1.7M solution (in ethanol) of DPPH for > 1hr with Ar, aliquots of the reagent were injected into vials containing 1 g material (stored under Ar). After shaking, material was separated from solution by centrifugation (10 min, 4500 rpm) and analysed on a Shimadzu UV mini 1240 UV/vis spectrophotometer using a 1cm path length. The mean, minimum and maximum percentage variation for duplicate measurements were 30%, 3.1% and 70% respectively (n=30).

50 suspended sediment samples were collected from the river draining Leverett Glacier in 2012 by centrifuging known volumes ( $\geq 100$  ml) of water at 4500 rpm for 10 minutes. Sets of 10 suspended sediments from different points in the melt season were combined to give enough material for surface area (BET) analysis.

## Calculations

### **H<sub>2</sub> production rate in the catchment of Leverett Glacier, SW Greenland, and comparison with previously measured rates of potential hydrogen oxidation via methanogenesis.**

We first calculate the H<sub>2</sub> generated from rock comminution on an annual basis via Equation (S1):

$$(S1) \quad H2_{annual} = \frac{H2 \times D \times M}{A \times 365}$$

where  $H_{2\text{annual}}$  is the amount of  $H_2$  generated from rock comminution in a year ( $\text{nmol m}^{-2} \text{a}^{-1}$ ),  $H_2$  is the amount of  $H_2$  produced per gram of suspended sediment ( $11.4 \text{ nmol g}^{-1}$ , using a mean surface area for suspended sediment of  $4.37 \text{ m}^2 \text{ g}^{-1}$  from Table S2, a mean molar silica content of 17.9 % from Table S1, and using the regression equation from Figure 1c),  $D$  is the annual discharge from the Leverett catchment over the 2012 melt season ( $2.65 \times 10^{12} \text{ L}$ )<sup>3</sup>,  $M$  is the mean concentration of suspended sediment over this same period ( $1.08 \text{ g L}^{-1}$ )<sup>3</sup>,  $A$  is the Leverett Glacier catchment size ( $6 \times 10^8 \text{ m}^2$ )<sup>4</sup>, and 365 converts the annual rate to a daily rate. These calculations give an estimated hydrogen generation rate from rock comminution under Leverett Glacier of  $150 \text{ nmol H}_2 \text{ m}^{-2} \text{ d}^{-1}$ . These calculations assume that 100% of the subglacial bed is at the pressure melting point (warm-based), with liquid water available to react with crushed mineral grains. If a substantial fraction of the bed was cold based, then rates of unit area  $H_2$  production would be accordingly higher. The assumption of a largely warm-based glacier is consistent with the widespread acceleration of ice velocity observed annually at Leverett Glacier following the onset of the surface melt season<sup>5</sup>.

We then calculate the  $H_2$  oxidation potential of previously measured rates of methanogenesis ( $0.18 \text{ pmol CH}_4 \text{ g}^{-1} \text{ d}^{-1}$ ) in subglacial sediments at Russell Glacier<sup>6</sup>. Russell Glacier is immediately adjacent to Leverett Glacier, overrunning similar bedrock and flowing from the same sector of the ice sheet<sup>6</sup>, and hence likely to sustain similar rates of microbial activity. These rates were measured at  $1^\circ\text{C}$  using a ratio of 8 ml of water to 2 g of subglacial sediment. First, we assume a 4:1 stoichiometry between  $H_2$  consumed and  $CH_4$  formed via Equation (S2) to give  $0.72 \text{ pmol H}_2 \text{ g}^{-1} \text{ d}^{-1}$



We then convert from mass normalised rates ( $H_{2_{\text{mass}}}$ ) to areal rates of potential microbial  $H_2$  oxidation ( $H_{2_{\text{ox}}}$ ) by Equation (S3), integrating to a 1 cm sediment thicknesses below the basal ice boundary.

$$(S3) \quad H_{2_{\text{ox}}} = H_{2_{\text{mass}}} \times \rho \times d \times 10$$

Where  $\rho$  is the density of Leverett subglacial wet sediment ( $2.0 \text{ g cm}^{-3}$ )<sup>6</sup>,  $d$  is an assumed depth of sediment in centimetres (1 cm), and  $\times 10$  converts units of  $\text{pmol H}_2 \text{ cm}^{-2} \text{ d}^{-1}$  to  $\text{nmol H}_2 \text{ m}^{-2} \text{ d}^{-1}$ . From Equation (S3), we estimate a potential microbial  $H_2$  oxidation rate via methanogenesis of  $14.4 \text{ nmol H}_2 \text{ m}^{-2} \text{ d}^{-1}$  integrated to a 1 cm thickness. The estimated  $H_2$  production from rock comminution under Leverett Glacier is therefore  $10.4\times$  more than the estimated potential hydrogen required to support rates of microbial methanogenesis in the top centimetre of sediment under the basal ice layer. These calculations indicate that rock comminution could support the measured rates of methanogenesis in the top layer of sediments below the basal ice boundary under warm based sections of the glacier.

### **Potential $\text{CO}_2$ and $\text{O}_2$ production from basal ice melt under Leverett Glacier**

To estimate the amount of  $\text{CO}_2$  and  $\text{O}_2$  available from basal ice melt under Leverett Glacier we assume a basal ice melt rate of  $6 \text{ mm yr}^{-1}$ <sup>7</sup>, equivalent to an ice volume of  $6 \text{ L m}^{-2} \text{ yr}^{-1}$ . If we assume a typical basal ice gas content of 10% vol./vol. and pre-industrial  $\text{CO}_2$  and  $\text{O}_2$  fractions of 0.0003 and 0.21<sup>8</sup>, then  $4.9 \times 10^{-7} \text{ L CO}_2 \text{ m}^{-2} \text{ d}^{-1}$  and  $3.5 \times 10^{-4} \text{ L O}_2 \text{ m}^{-2} \text{ d}^{-1}$  would be released from air inclusions under Leverett Glacier. Using the Ideal Gas Law ( $PV = nRT$ ,

where R is  $0.08205736 \text{ L atm K}^{-1} \text{ mol}^{-1}$ ) this is equivalent to  $22 \text{ nmoles CO}_2 \text{ m}^{-2} \text{ d}^{-1}$  and  $15.4 \text{ } \mu\text{moles O}_2 \text{ m}^{-2} \text{ d}^{-1}$  respectively. Together, these are more than sufficient to oxidise the estimated  $\sim 150 \text{ nmoles H}_2 \text{ m}^{-2} \text{ d}^{-1}$  produced from rock comminution under Leverett Glacier.

### **Microcosm and phylogenetic analysis at Robertson Glacier**

**Microcosm experiments.** Subglacial sediments were sampled aseptically from an ice cave that developed due to the flow of the western meltwater stream (termed RW) at the terminus of Robertson Glacier in July 2008. Details of sediment sampling and preservation during transit to the laboratory are as reported previously<sup>9</sup>. Sediments were kept frozen ( $-20^\circ\text{C}$ ) until used to initiate microcosm assays. Ten grams of wet subglacial sediment fines ( $\sim 8.2 \text{ gdw}$ s) were added to sterilized 70 mL serum bottles and overlaid with 10 mL of anaerobic, filter sterilized ( $0.22 \text{ } \mu\text{m}$ ) phosphate buffered (5 mM) distilled water (pH 7.5). Triplicate microcosms were degassed with sterile  $\text{N}_2$  passed over heated reduced copper shavings to remove residual  $\text{O}_2$ . Anaerobic microcosms were amended with acetate (5 mM final concentration), methanol (5 mM final concentration), a headspace of  $\text{H}_2/\text{CO}_2$  (80/20% vol./vol.), or nothing (unamended control). For each condition above triplicate microcosms were prepared that contained bromoethansulfonate (BES; 10 mM final concentration) or methyl fluoride (0.5% vol./vol. final concentration in the gas phase) as inhibitors of all methanogens and acetoclastic methanogens, respectively. The final step in preparation of microcosms was amendment with cysteine hydrochloride (pH 7.5) to a final concentration of 0.5% wt./vol. A SRI 8610C gas chromatogram equipped with a flame ionization detector and methanizer was used to assess production of  $\text{CH}_4$  over the course of the incubation. Helium was used as the carrier gas and

a Restek Porapak Q SS (1.8 m) column was used for separation of CH<sub>4</sub>, using a 1 mL sample loop. Peak areas were integrated using Peak Simple™ software using certified gas standards American Gas Group (Toledo, Ohio).

**Phylogenetic Analysis.** Archaeal 16S rRNA genes were amplified and sequenced from RG subglacial sediments as a part of our previous study<sup>9</sup>. The phylogenetic position of representative archaeal OTUs (defined at 97% sequence identities) was evaluated by approximate likelihood-ratio tests<sup>10</sup> as implemented in PhyML-aBayes (version 3.0.1)<sup>11</sup>. The archaeal 16S rRNA gene phylogeny was rooted with 16S rRNA genes from the crenarchaeotes *Acidilobus sulfurireducens* (EF057391) and *Caldisphaera draconis* (EF057392). Phylogenies were constructed using the General Time Reversible (GTR) substitution model with a proportion of invariable sites and gamma-distributed rate variation as recommended by jModeltest (ver. 3.8)<sup>12</sup>. Sequences that that comprised lineages denoted as “phylotype I” and “phylotype II” are indicated.

**Phylotype Primer Design and Quantitative PCR.** RG sediment-associated archaeal 16S rRNA genes obtained as a part of our previous study<sup>8</sup> were compiled and aligned as previously described<sup>12</sup>. Alignments were used to identify regions of the 16S rRNA gene that demarcated these two phlotypes. Primer Phylo-IF (5'-ACCGATGGCGAAGGCATCCC-3') and Phylo-IIF (5'-ACCTGTGGCGAAGGCGTCTTA-3') were used in conjunction with the archaeal reverse primer 958R (5'-YCCGGCGTTGAMTCCAATT-3') to selectively amplify phlotypes I and II, respectively. Generated amplicons were ~ 250 bp. PCR conditions were the same as previously described with the exception that the annealing temperature for Phylo-IF-958R primer set was 62.7°C and the annealing temperature for Phylo-IF-958R primer set

was 61.7°C. Specificity of each primer pair was checked using plasmid DNA containing inserts from the phylotype not targeted for amplification.

Quantitative PCR (qPCR) was used to estimate the number of templates that were affiliated with phylotype I and II in *i*) sediments used to initiate the microcosms and *ii*) sediments sampled from microcosms following 494 days of incubation. Sediments were subjected to nucleic acid extraction and quantification as previously described<sup>9</sup>. Methods for qPCR generally followed our previously described methods<sup>13</sup> and used archaeal 16S rRNA plasmids, generated as part of our previously described study<sup>9</sup>, to generate standard curves. qPCR assays were performed in a Rotor-Gene 300 quantitative real-time PCR machine (Qiagen, Valencia, CA) in 0.5 mL optically clear PCR tubes (Qiagen, Valencia, CA) using a SsoFast<sup>TM</sup> EvaGreen Supermix qPCR Kit (Bio-Rad Laboratories, Hercules, CA). qPCR assays were amended with molecular-grade bovine serum albumin (Roche, Indianapolis, IN) to a final concentration of 0.4 mg ml<sup>-1</sup>. qPCR cycling conditions were as follows: initial denaturation (95°C for 10 min) followed by 40 cycles of denaturation (95°C for 10s), annealing at defined temperatures (see above), and extension (72°C for 20 s). Specificity of the qPCR assays was verified by melt curve analysis. Negative control assays were performed in the absence of template DNA. Each assay was performed in triplicate and the reported template abundances are the average and standard deviation of triplicate determinations.

## References

- 1 Wiesenburg, D. A. & Guinasso Jr., N. L. Equilibrium solubilities of methane, carbon monoxide, and hydrogen in water and sea water. *Journal of Chemical and Engineering Data* **24**, 356-360 (1979).
- 2 Damm, C. & Peukert, W. Kinetics of Radical Formation during the Mechanical Activation of Quartz. *Langmuir* **25**, 2264-2270 (2009).
- 3 Hawkings, J. R. *et al.* Ice sheets as a significant source of highly reactive nanoparticulate iron to the oceans. *Nature Communications* **5**, 3929-3929 (2014).
- 4 Cowton, T., Nienow, P., Bartholomew, I., Sole, A. & Mair, D. Rapid erosion beneath the Greenland ice sheet. *Geology* **40**, 343-346 (2012).
- 5 Cowton, T. *et al.* Evolution of drainage system morphology at a land-terminating Greenlandic outlet glacier. *Journal of Geophysical Research-Earth Surface* **118**, 29-41 (2013).
- 6 Stibal, M. *et al.* Methanogenic potential of Arctic and Antarctic subglacial environments with contrasting organic carbon sources. *Global Change Biology* **18**, 3332-3345 (2012).
- 7 Breemer, C. W., Clark, P. U. & Haggerty, R. Modeling the subglacial hydrology of the late Pleistocene Lake Michigan Lobe, Laurentide Ice Sheet. *Geological Society of America Bulletin* **114**, 665-674 (2002).
- 8 Souchez, R., Lemmens, M. & Chappellaz, J. Flow-induced mixing in the GRIP basal ice deduced from the CO<sub>2</sub> and CH<sub>4</sub> records. *Geophysical Research Letters* **22**, 41-44 (1995).



- 9 Boyd, E. S., Skidmore, M., Mitchell, A. C., Bakermans, C. & Peters, J. W. Methanogenesis in subglacial sediments. *Environmental Microbiology Reports* **2**, 685-692 (2010).
- 10 Anisimova, M. & Gascuel, O. Approximate likelihood-ratio test for branches: A fast, accurate, and powerful alternative. *Systematic Biology* **55**, 539-552 (2006).
- 11 Anisimova, M., Gil, M., Dufayard, J. F., Dessimoz, C. & Gascuel, O. Survey of branch support methods demonstrates accuracy, power, and robustness of fast likelihood-based approximation schemes. *Systematic Biology* **60**, 685-699 (2011).
- 12 Darriba, D., Taboada, G. L., Doallo, R. & Posada, D. jModelTest 2: more models, new heuristics and parallel computing. *Nature Methods* **9**, 772-772 (2012).
- 13 Boyd, E. S. *et al.* Diversity, abundance, and potential activity of nitrifying and nitrate-reducing microbial assemblages in a subglacial ecosystem. *Applied and Environmental Microbiology* **77**, 4778-4787 (2011).

## SUPPLEMENTARY INFORMATION

### Rock comminution as a source of hydrogen for subglacial ecosystems

J. Telling<sup>1\*</sup>, E.S. Boyd<sup>2</sup>, N. Bone<sup>1</sup>, E.L. Jones<sup>1</sup>, M. Tranter<sup>1</sup>, J.W. MacFarlane<sup>3</sup>, P.G. Martin<sup>3</sup>, J.L. Wadham<sup>1</sup>, G. Lamarche-Gagnon<sup>1</sup>, M.L. Skidmore<sup>4</sup>, T.L. Hamilton<sup>5</sup>, E. Hill<sup>6</sup>, M. Jackson<sup>7</sup> and D.A. Hodgson<sup>8</sup>

#### Tables

**Table S1.** Mean molar composition (%) of mineral, rock and suspended sediment samples (bd denotes below detection, IC is inorganic carbon, OC is organic carbon).

Molar %	Calcite	Leverett Glacier gneiss	Leverett Glacier suspended sediment	Robertson Glacier shale	Ellsworth Mt. quartzite	Mitivakkat Glacier granite	Kiattuut Sermiat Glacier nepheline-syenite	Engabreen schist
<b>O</b>	54.9	57.9	54.2	53.9	58.2	51.9	50.8	51.9
<b>Ca</b>	21.4	1.18	2.37	9.46	0.42	1.79	1.23	0.76
<b>Si</b>	bd	22.1	17.94	11.1	23.2	20.8	21.9	17.7
<b>Mg</b>	bd	0.56	2.46	4.15	0.79	2.27	0.27	4.16
<b>Al</b>	bd	8.29	8.45	3.55	5.84	9.53	7.63	11.0
<b>K</b>	bd	2.69	1.60	2.05	1.53	1.87	3.21	4.29
<b>Fe</b>	bd	0.46	3.18	0.59	1.85	2.15	3.16	3.15
<b>Na</b>	bd	5.27	3.58	0.65	4.16	3.59	5.41	0.75
<b>Ti</b>	bd	bd	0.92	bd	bd	0.48	0.58	0.73
<b>N</b>	bd	bd	bd	0.1	bd	bd	bd	bd
<b>H</b>	bd	1.26	1.49	3.83	3.90	4.58	4.17	4.56
<b>IC</b>	21.6	0.21	3.72	8.05	0.09	0.16	0.32	0.14
<b>OC</b>	2.14	bd	0.07	2.5	0.02	bd	bd	bd

**Table S2.** Details of suspended sediment samples collected from the subglacial outlet stream at Leverett Glacier during summer 2012 and used for surface area measurements.

Dates of sampling (all represent 10 combined samples)	Surface Area m <sup>2</sup> g <sup>-1</sup>
17.6.12 to 30.6.12	5.42
3.7.12 to 5.7.12	3.33
8.7.12 to 11.7.12	5.42
24.7.12 to 29.7.12	4.00
4.8.12 to 6.8.12	3.65
<i>Mean</i>	$4.37 \pm 0.82 (1\sigma)$

## Figures

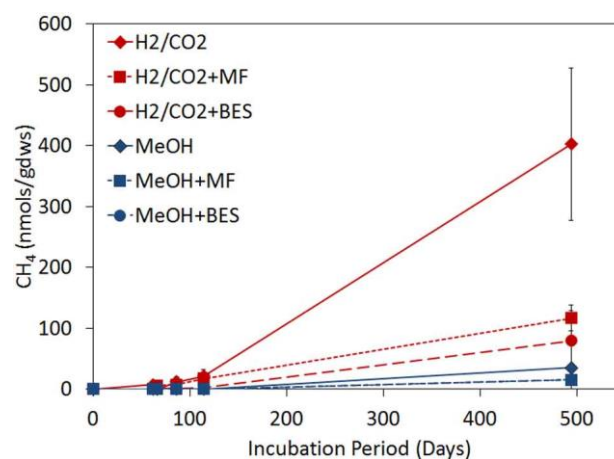


**Figure S1.** Production of methane in microcosms amended with various nutrients and inhibitors. Unamended microcosms and those amended with acetate are not shown as methane was always below the limit of detection in these assays. Abbreviations: MF, methyl fluoride;

BES, bromoethanesulfonate; MeOH, methanol. The partial inhibition of hydrogenotrophic methanogenesis by MF is consistent with previous studies that have shown these organisms to be sensitive to MF but not fully inhibited<sup>1</sup>.

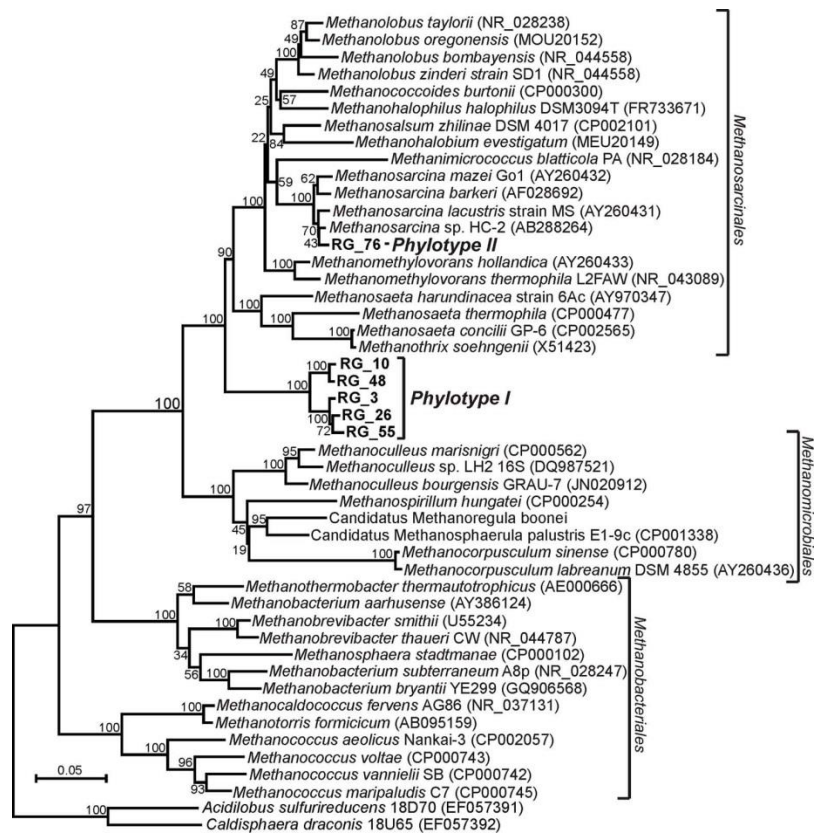


**Figure S2.** Maximum likelihood phylogenetic reconstruction of archaeal 16S rRNA genes recovered from RG subglacial sediments. Sequences comprising “phylotype I” and “phylotype II” are indicated.

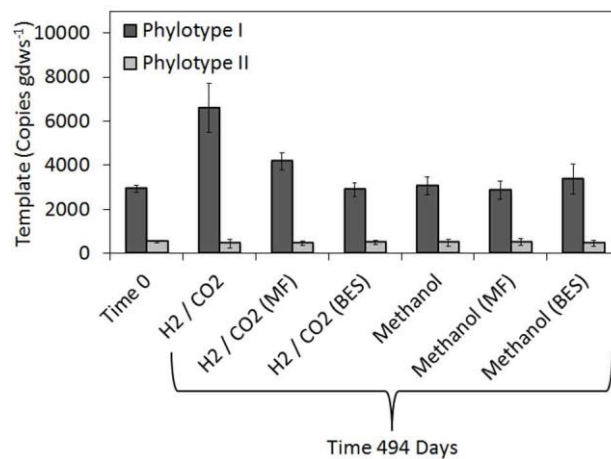


**Figure S3.** Abundance of 16S rRNA genes associated with phylotype I and II in subglacial sediments used to inoculate microcosm incubations (denoted as time 0) and sediments collected after 494 days of incubation. Abbreviations: MF, methyl fluoride; BES, bromoethanesulfonate.

## References

1. Conrad R. & Klose M. How specific is the inhibition by methyl fluoride of acetoclastic methanogenesis in anoxic rice field soil? *FEMS Microbiology Ecology* **30**, 47-56 (1999).